ISBN: 978-3-95450-208-0 doi:10.18429/JACoW-IPAC2019-MOPTS104

A TOOLKIT FOR TRACING ELECTRON BEAM ENVELOPE AT LOW ENERGY SECTION OF TPS LINAC

H. H. Chen, H. C. Chen, Y. K. Lin, K.-K. Lin , NSRRC, Hsinchu, Taiwan

Abstract

Based on calculated Bz of solenoids installed at the TPS linac low energy section, the electron beam envelope along beam centerline has been explored in this work using the initial and boundary conditions provided in the linac specifications. Concept of magnetic flux compression is adopt to analyze the beam size variation along linac centerline. The calculated result of selected checkpoints has been experimentally verified using screen monitors. In order to benefit tuning capability in routine operation, the display of beam size variation along centerline is integrated into the previously developed toolkit 'linac'. It is hope that it will provide an interactive approach for linac tune-up process and would be helpful to its routine operation.

INTRODUCTION

The efficiency of linear accelerator is known from operation experience, that is, the survival rate of the electron beam from the electron gun to the lineal accelerator is closely related to the set value of the coil current in the low energy section. In order to improve the tuning capability of linear accelerator, it is an important task to discuss the operation parameters and perform the verification. By means of interactive software design and verification, the motion of electron beam under different magnetic field conditions is studied.

First, according to the coil magnetic field setting and the initial conditions for the electron beam to leave the electron gun, the transverse (perpendicular to the centerline) beam size at the low energy section (<10 MeV) is simulated using the self-developed software. Then the size of the electron beam is measured by several screen monitors at specific positions, and the measured data is verified by comparison with the simulation and calculation results. The results show that the numerical value of the software simulation is close to the actual measured value, so the calculation function of the electron beam size is integrated into the simulation program. The physical principles used in the simulation calculation and the various functions of the software toolkit are presented in the report.

MAGNETIC FIELD DISTRIBUTION

In the low energy section, the electron beam moves along the direction of the magnetic field, while the transverse electron beam size is limited by the applied magnetic flux compression. The adjustable knob of the interactive software can provide the variation of the centerline magnetic field, describe the size of the electron beam in different centerline positions by the distribution of the magnetic field, and make comparison with the actual experimental observation.

The electron beam leaves the electron gun exit with an energy of 90 KeV as shown in Figure 1. When passing through prebuncher and final buncher, it obtains energy of 300 KeV and 3 MeV respectively, and then the electron beam enters the first low energy section of the linear accelerator. The electron beam energy is less than 10 MeV in the section and it is about 1/5 of the length of the front end of the first acceleration tube. The electron beam energy has reached 10 MeV and it is no longer necessary to use the focus coil magnetic field.

The initial and boundary conditions for this study are listed as follows: [1]

- The electron beam leaves the electron gun with an energy of 90 KeV, and its normalized emittance is $\varepsilon_n = 50\ (\pi)\ \text{mm} \cdot \text{mrad}$.
- When the electron beam passes through the buncher, its energy increases from 90 KeV to 3 MeV.
- The magnetic field of the focus coil is solved with hard-edge condition to simplify the calculation.

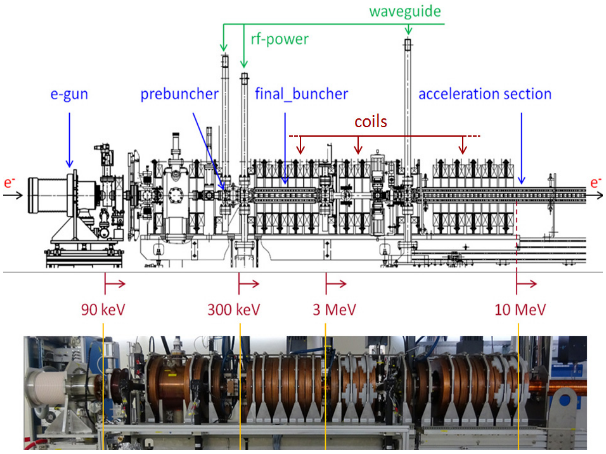

Figure 1: TPS linac buncher.

MAGNETIC FLUX COMPRESSION

When the electron beam meets the initial and boundary conditions listed in the second section, and the energy is less than 10MeV before the electron beam enters the linear accelerator, its transverse size will comply with the centerline magnetic flux compression law. This is why the magnetic flux compression law in the report is used to calculate the transverse size of the electron beam and to analyze the state of the electron beam after leaving the electron gun before entering the linear accelerator [2] and the magnetic flux conservation law is also used in electron beam cross-section calculation [3].

EVOLUTION OF ELECTRON BEAM ENVELOPE

According to the magnetic field setting conditions under daily operation, the magnetic field along the centerline of buncher is calculated, as shown in Figure 2. Red dotted line shows the screen monitor position. The parameter profile of the daily operation conditions was also used in the simulation study in this report. Although the electron beam energy is increased from 90 KeV to 3 MeV, and then to 10 MeV after entering the linear accelerator, the size of the electron beam with lower energy less than 10 MeV at a specific position can be calculated and compared by using the magnetic flux compression law [4].

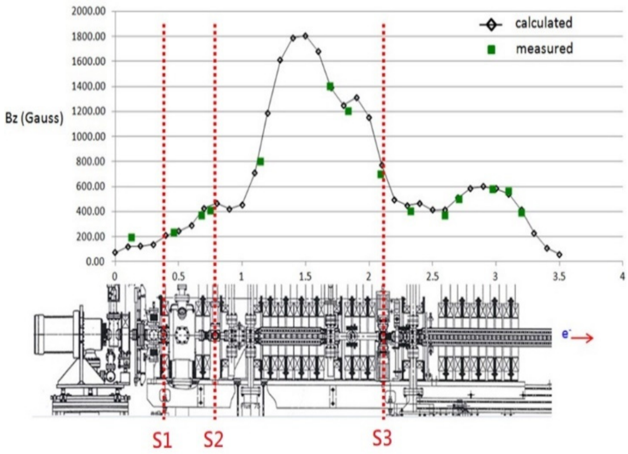

Figure 2: Magnetic field condition of daily operation.

ELECTRON BEAM MEASUREMENT

The three screen monitors S1/S2/S3 at specific positions are shown in Figure 2. The coil current setting for measurement is consistent with that used in daily operation. The electron beam size displayed by the screen monitor during measurement is shown in Figure 3. The actual size of the electron beam can be obtained by the size of the electron beam displayed on the screen.

The centerline position, measured electron beam size and measured magnetic field are listed in Table 1. The product of the calculated magnetic field and the size square of the electron beam is listed in the last column to verify the conservation of magnetic flux. According to the calculation results in the last column, although the B_zR^2 values of 0.8m and 2.1m in the centerline position are different, they still show some errors through the screen. According to the measured results, there is an error of about 0.1~0.3mm, so the measured results in these two places should conform to the conservation of magnetic flux. The B_zR^2 value at the axial position of 0.4m is obviously significantly different from the other two results, which should be attributed to the fact that this position happens to be located at prebuncher, where the electron beam is greatly affected by the buncher, so the result is not consistent with the conservation of magnetic flux.

Table 1: Measured Electron Beam Size

Screen	**S1**	**S2**	**S3**
Centerline position (m)	0.4	0.8	2.1
Electron beam radius R (mm)	2.92	2.64	1.83
Centerline field B_z (Gauss)	230	410	700
B_zR^2 (Gauss · m^2)	1961	2857	2344

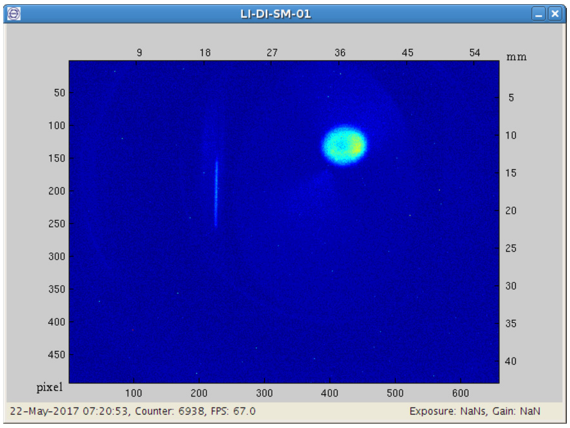

22-May-2017 07:20:53, Counter: 6938, FPS: 67.0 Exposure: NaNs, Gain: NaN

Figure 3: Electron beam displayed on S1 screen monitor.

ELECTRON MOTION IN FIELD

The schematic diagram of electrons gyrating forward in the magnetic field is shown in Figure 4. The radius of gyration is called Larmor radius [5]. Considering that when the electron beam leaves the electron gun, its normalized emittance is ε_n = 50 (π) mm · mrad, the geometrical emittance of the electron beam at different energies can be calculated by the equation $\varepsilon_n = \beta\,\gamma\,\varepsilon_g$. and are normalized emittance and geometrical emittance. β is ratio of electron and light velocity. γ is ratio of electron relativistic energy and rest mass energy [6].

The electron energy after leaving the electron gun is 90 KeV, and the electron transverse forward momentum ratio is about 1.5E-2. For the different stages of electron energy, the corresponding β and γ values can be calculated, and the electron transverse forward momentum ratio is related to the electron energy. In the calculation, the electron transverse velocity in the low-energy section (less than 10MeV) is not changed, so the electron transverse forward momentum ratio is related to the electron energy. The Larmor radius values were calculated by electron transverse forward momentum ratio and magnetic field B_z are shown in Table 2.

Table 2: Calculated Larmor Radius

Screen	**S1**	**S2**	**S3**
Electron energy (MeV)	0.09	0.09	3
Electron transverse forward momentum ratio	1.5E-2	1.5E-2	5E-4
Centerline field Bz (Gauss)	230	410	700
Larmor radius (mm)	0.2	0.1	2.2
Electron beam radius R (mm)	2.92	2.64	1.83

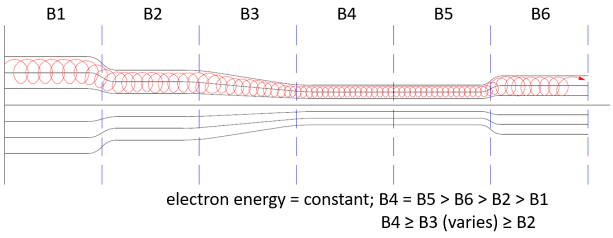

Figure 4: Illustration of magnetic flux compression and Larmor radius.

In the practical case of TPS-linac discussed in this report, the results of the relevant values show that the radius of gyration of the electron beam on the S1/S2 screens is far less than the size of the electron beam calculated by magnetic flux compression, so the Larmor radius can be ignored in the measurement of the electron beam transverse cross-section. However, the Larmor radius at screen S3 is larger than the measured cross-section of the electron beam. It is speculated that this part should be related to the boundary setting during calculation, and further experimental evaluation is needed to explain the irrationality of this part.

ELECTRON BEAM CROSS-SECTION SIMULATION

The simulation program uses the TPS linear accelerator focus coil parameters to calculate the centerline magnetic field distribution and then uses the magnetic flux conservation law to calculate the electron beam size at different centerline positions. The radius of the electron beam leaving the electron gun is 5mm. Because the position of the sub-harmonic buncher is between 0.4 and 0.7m, the electron beam passing through this section is affected by the buncher, resulting in a large error between the actual measurement value and the simulation result.

The red line in Figure 5 is the simulated electron beam size distribution and the blue line is the magnetic field distribution. The simulation program contains an interactive function that can select several focus coils to simultaneously increase or decrease the current to observe the distribution of magnetic field and electron beam size.

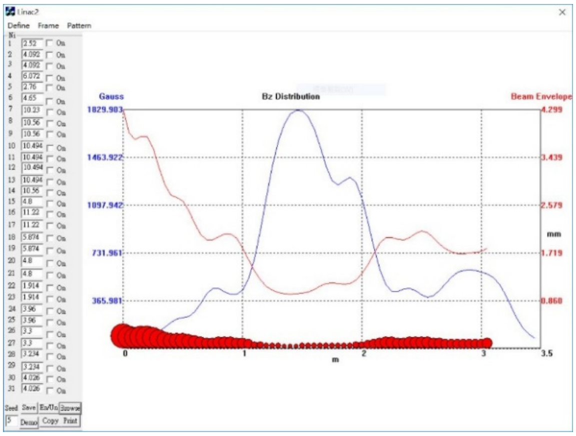

Ni		
1	2.52	☐ On
2	4.092	☐ On
3	4.092	☐ On
4	6.072	☐ On
5	2.76	☐ On
6	4.65	☐ On
7	10.23	☐ On
8	10.56	☐ On
9	10.56	☐ On
10	10.494	☐ On
11	10.494	☐ On
12	10.494	☐ On
13	10.494	☐ On
14	10.56	☐ On
15	4.8	☐ On
16	11.22	☐ On
17	11.22	☐ On
18	5.874	☐ On
19	5.874	☐ On
20	4.8	☐ On
21	4.8	☐ On
22	1.914	☐ On
23	1.914	☐ On
24	3.96	☐ On
25	3.96	☐ On
26	3.3	☐ On
27	3.3	☐ On
28	3.234	☐ On
29	3.234	☐ On
30	4.026	☐ On
31	4.026	☐ On

Seed: 5

Figure 5: The simulated electron beam size and magnetic field distribution.

In addition, by selecting Pattern>Ellipse at the function key of the simulation program, the pie chart information of the electron beam transverse cross-section can be displayed in addition to the magnetic field and electron beam size distribution. The correlation between magnetic field change and electron beam cross-section size can be clearly compared through the change of electron beam cross-section size, as shown in Figure 5.

CONCLUSION

The electron beam size data comparison between the simulation program and measurement with the screen monitor shows high coincidence as Figure 6. At the S1 screen monitor position, there is a large error between the simulation and measurement values, which is judged to be affected by the prebuncher.

The evaluation of simulation program and the actual measurement shows that the real-time electron beam size simulation is not only useful for daily operation but also for further understanding on acceleration mechanism. It is worthy to develop the related functions to be a useful electronic control assistant toolkit.

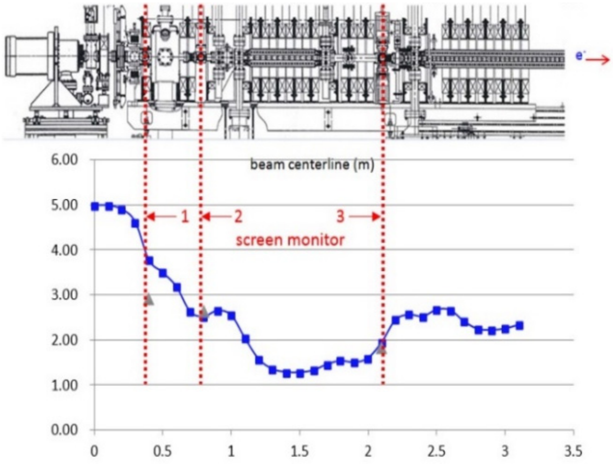

Figure 6: Electron beam size between simulation and measurement.

REFERENCES

[1] K. L. Tsai, C. S. Fann, H. M. Shih, K. K. Lin, "TPS linac acceptance tests verification of compliance to specifications," NSRRC-linac-2011-04.

[2] K. Dunkel, ACCEL report: "150 MeV linac design for TPS," A-BP-7426-A, June 20, 2008.

[3] P. Lorrain, D.R. Corson, "Electromagnetic fields and waves," 2nd edition, W.H. Freeman and Company, 1972, p. 381.

[4] H. H. Chen *et al.*, "Bz Calculation of TPS Linac Focusing Coils and a Toolkit for Bz Optimization", in *Proc. 8th Int. Particle Accelerator Conf. (IPAC'17)*, Copenhagen, Denmark, May 2017, pp. 4321-4323. `doi:10.18429/JACoW-IPAC2017-THPIK098`

[5] Francis F. Chen, Introduction to plasma physics, 1974 Plenum Press, New York, USA, p. 18.

[6] Peace Chang *et al.*, "Tracing of electron beam envelope at low energy section of TPS linac", NSRRC-linac-2018-04.